JOURNAL OF AIRCRAFT
Vol. 31, No. 1, Jan.–Feb. 1994

Control of Cavity Flow by Upstream Mass-Injection

Ahmad D. Vakili* and Christian Gauthier†
University of Tennessee Space Institute, Tullahoma, Tennessee 37388

The purpose of this study was to use mass-injection upstream of a cavity to control the shear flow across the cavity for reducing or eliminating cavity flow oscillations. Results of an experimental effort performed at a nominal Mach number of 1.8 and at unit Reynolds number of 17 × 10^6 per foot for a cavity with length-to-depth (L/D) ratio of 2.54 are presented. Baseline measurements were performed for various mass-injection rates for two rectangular injection distributions. Significant attenuation of cavity oscillations was observed with upstream mass-injection. This was attributed to the thickening of the cavity shear layer, which altered its instability characteristics, such that its preferred vortex roll-up frequency was shifted outside of the natural frequencies of the cavity. As a result of the experimental investigation, it was concluded that mass-injection is effective in significantly reducing or eliminating cavity oscillations. Cavity's peak oscillation amplitude was reduced from about 174 dB (1.5 psi) without mass-injection to 147 dB (0.07 psi) at the blowing coefficient rate of 0.04.

I. Introduction

FLOW over cavities is encountered in a wide range of aerodynamic vehicle applications, including weapon bays, wheel wells, control slots, and optical window openings. Under certain conditions, large flow and pressure oscillations occur within these cavities. In weapon bay cavities, these oscillations are of great concern when carrying and separating stores. The oscillations also result in undesirable increases in the vehicle's aerodynamic noise and drag, as well as structural vibration and fatigue. Because of these issues, the subject of cavity flow has been extensively studied. In general, cavity flow can be divided into the following three categories based on the cavity length-to-depth (L/D) ratio[1]: 1) closed cavity flow—for $L/D > 13$, flow attaches to the bottom of the cavity; 2) open cavity flow—for $L/D < 8$, flow spans the cavity without attaching to the bottom; and transitional cavity flow—for $8 < L/D < 13$, flow may behave as in either a closed or an open cavity flow; or in fact, it may be unstable and alternate between the two modes. Among these, the category of open cavity flow can additionally exhibit either lengthwise (longitudinal) or depthwise (normal) modes of oscillations based, generally, upon the longest cavity dimension. In open cavity flows, longitudinal modes of oscillations usually dominate for shallow cavities, i.e., with a L/D ratio greater than one, while normal modes dominate in deep cavities.

Open cavity flow in shallow cavities is typically encountered in weapon bay applications. In this flow, the longitudinal pressure and flow oscillations have been associated to the shear layer interactions with the cavity. As explained by a self-exciting feedback mechanism, perturbations are produced when the shear layer interacts with the cavity trailing edge. These perturbations travel upstream within the cavity and eventually excite the shear layer at the cavity leading edge. As a result of these excitations, the shear layer development along the cavity is altered, and consequently, the subsequent interactions at the trailing edge are also affected. The whole feedback process is, therefore, continuously altered. Whenever proper timing exists between these events, the feedback process can lead to resonance and result in a large amplification of the cavity oscillations at certain frequencies.

This feedback model permits a fairly accurate determination of all the possible longitudinal modes of cavity oscillations for open cavity flow in shallow cavities. However, models of cavity oscillations are limited because of the incomplete understanding of the shear layer feedback mechanisms. Tam and Block[2] have pointed to the lack of a complete understanding as to how the pressure waves are created at the cavity trailing edge.

Heller et al.[3] improved upon Rossiter's semiempirical formula. The resulting modified Rossiter's formula presented below agrees well with supersonic test data as indicated by Fig. 1

$$S = \frac{fL}{U_0} = \frac{(m - n)}{\left\{ \dfrac{M}{\left[1 + \dfrac{(\gamma - 1)}{2} M^2\right]^{1/2}} + \dfrac{1}{K_v} \right\}} \tag{1}$$

where γ is the specific heat ratio, S is the Strouhal number based on the cavity length L, the frequency f, and the freestream velocity U_0; M is the freestream Mach number; m is an integer mode number (which accounts for the number of waves involved); K_v and n are empirical constants representing the vortices convective velocity (as a ratio to the freestream velocity) and a rear corner interaction time delay, respectively. The modified Rossiter's formula only predicts possible frequencies of oscillation. It remains practically impossible to predict which mode or what amplitude of oscillations will occur in a cavity; in fact, it is not even possible to determine if there will be any oscillations.

As a result of this incomplete understanding, nearly all techniques investigated for the suppression of cavity oscillations have only been partially effective. They generally consist of passive disturbances which only reduced the cavity oscillations at specific "design" conditions.[4,5] Some techniques altered the characteristics of the oncoming shear layer by using devices such as vortex generators and sawtooth spoilers. Other techniques attempted to stabilize the shear layer impinging point at the cavity trailing edge by using geometric ramps and trailing edge cowls.[4,5]

Various mechanisms have been investigated including mass-injection from the cavity base (ceiling). Sarohia and Massier[6]

Presented as Paper 91-1645 at the AIAA 22nd Fluid and Plasmadynamics Conference, Honolulu, HI, June 24–26, 1991; received July 16, 1991; revision received Feb. 4, 1993; accepted for publication Feb. 5, 1993.

*Associate Professor, Aerospace/Mechanical Engineering. Associate Fellow AIAA.
†Graduate Research Assistant. Member AIAA.

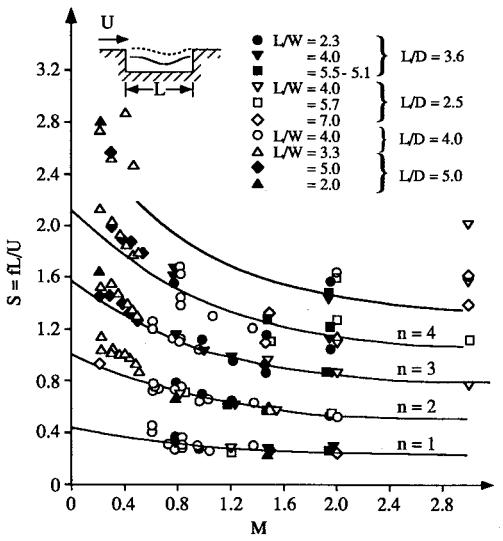

Fig. 1 Strouhal number variations ($S = fL/U$) with Mach number for different modes of open cavity flows. Symbols are experimental data,[3] lines are Eq. (1).

found that mass-injection from the base resulted in a reasonable reduction (8–10 dB) of the peaks, with blowing parameter B_e of approximately 0.05–0.15, where the blowing parameter is defined by the ratio of the injected mass flux to the freestream mass flux $B_e \equiv \rho_w U_w/\rho_e U_e$. Franke and Sarno[7] used mass-injection through a slit from the leading edge of the cavity at different angles. Franke and Sarno obtained approximately a 10-dB sound pressure level reduction by blowing at 45 deg at the leading edge of the cavity, at a mass flow rate of 1.5 lbm/ft/s. This approach is equivalent to the spoiler concept with the spoiler being replaced by a jet sheet. In addition, this concept can be implemented as an active or even an adaptive control technique. Wilcox[8,9] used passive venting, by moving high-pressure air to the low-pressure region of the cavity, through a porous cavity floor to reduce the cavity flow interactions with the weapons during separation. Stallings and Forrest[10] used vent pipes to do the same with limited success. Recent computations of a similar approach, by Chokani and Kim,[11] found reduced amplitudes in the cavity.

Active shear layer flow control such as upstream mass-injection has been considered as a means to actively modify the characteristics of the shear layer just ahead of the cavity. This concept was investigated in a qualitative water table study by Vakili et al.[12] and Taylor.[13] Steady mass-injection produced significant attenuation of the cavity oscillations. Out-of-phase pulsed mass-injection nearly eliminated the oscillations initially, while after a shift in the frequency response of the cavity the oscillations were excited to a higher amplitude. With their experiment the potential use of upstream mass-injection for the attenuation of cavity oscillations was qualitatively demonstrated.

The present study was carried out in two steps. In the first step, "baseline" characteristics of the tunnel flow and the cavity flow are established for the empty tunnel and for no upstream mass-injection, respectively, by measuring the flow properties, frequencies, and amplitudes of the cavity oscillations. In the second step, similar measurements were conducted for various mass-injections for two perforation distributions. The effects of upstream injection on cavity oscillations are determined through comparison of the flow properties with and without mass-injection.

II. Mass-Injection: A Brief Review

The influence of mass-injection on the external flow depends upon the relative momentum of the injected mass to the freestream and varies from localized boundary-layer interactions to global interactions. As such, mass-injection may be categorized[14] in the following three categories:

A. Weak Mass-Injection

The effects of weak mass-injection are constrained to the boundary layer, affecting mostly the sublayer by shifting the logarithmic portion of the law of the wall (in turbulent flow). When the injected flow momentum is small, the boundary-layer thickness increases slowly over a relatively long distance, and the external flowfield is not substantially altered. This type of injection has been studied mostly for its effect upon skin friction or heat transfer when applied toward drag reduction and transpiration cooling, respectively.

B. Massive Mass-Injection

Massive mass-injection is sufficient to result in large external flow deflections. When the injectant momentum is much larger than the skin friction (but still much smaller than the external flow momentum), the external flow and original boundary layer are lifted above the injectant fluid, and a mixing layer is formed between the two fluids. This type of mass-injection has been used in attempts to simulate the mass addition resulting from ablative materials on re-entry vehicles.

C. Blowoff Mass-Injection

The injectant fluid momentum is comparable to the external flow momentum and the injectant is "blown-off" the wall as in a cross-jet. This type of interaction is mostly used for fuel injections applications and will not be considered in this study.

Two-dimensional models are based on the assumption that under moderate amounts of massive mass-injection the injected flow deflects the supersonic external flow uniformly to form a two-dimensional deflection wedge. It is also assumed that most viscous mixing effects are constrained to the mixing layer between the external and injected flows and, in turn, it is assumed that this layer is relatively small enough to be approximated by a so-called "dividing streamline."

Based on these assumptions, Bott[15] used a simple control volume approach to obtain an empirical relation between the injected wedge angle and the mass-injection rate. Fernandez and Zukoski[14] used a rigid theoretical approach to represent the injected flow region. They used the boundary-layer momentum equation, reduced in the form of the momentum thickness over a flat plate, to analyze this flow region:

$$\frac{d\theta}{dx} = \frac{C_f}{2} \tag{2}$$

On a flat plate with mass-injection another term is added to account for the injected flow relative momentum. If we define B_e as the ratio of the injected mass flow to the external or freestream mass flow, then $B_e = \rho_w V_w/\rho_e V_e$ and Eq. (2) becomes

$$\frac{d\theta}{dx} = \frac{\rho_w V_w}{\rho_e V_e} + \frac{C_f}{2} = B_e\left(1 + \frac{C_f}{2B_e}\right) \tag{3}$$

Under massive injection, however, it is assumed that the injection term is much larger than the friction term ($B_e >> C_f$), thus

$$\frac{d\theta}{dx} = B_e \tag{4}$$

The correlation between Fernandez's experimental results and the above equations is reasonable for most mass flows used. However, for larger mass flows, which result in an injection wedge angle above about 15 deg, Fernandez observed that the external flow curvature encountered usually only at the rear edge of the injection wedge occurred further and

further upstream. In this situation, the flow does not have self-similar velocity profiles and forms a curved wedge. Also, for these large wedge angles, Fernandez observed a separation region ahead of the injection zone because of the viscous and shock interactions.

From the momentum thickness growth calculations, Eq. (4), a boundary-layer-thickness-to-momentum-thickness ratio δ/θ had to be assumed to convert the results into an injected wedge growth, and subsequently, into an injected wedge angle. According to Fernandez, the δ/θ ratio decreases from 13 at low injection rates, to about 10 at higher injection rates. Results for various δ/θ, various initial momentum thickness θ_0 and various injection lengths L_{inj} are included in Fig. 2.

As shown in Fig. 2a, the length of injection has the greatest effect upon the induced wedge angles. However, mass-injection results are usually made independent of the length of injection by using the nondimensional B_e defined earlier. In these calculations, various injection lengths were used to study that effect directly, primarily to indicate that there are many ways to obtain either the same injected wedge angles or the same shear layer momentum thickness.

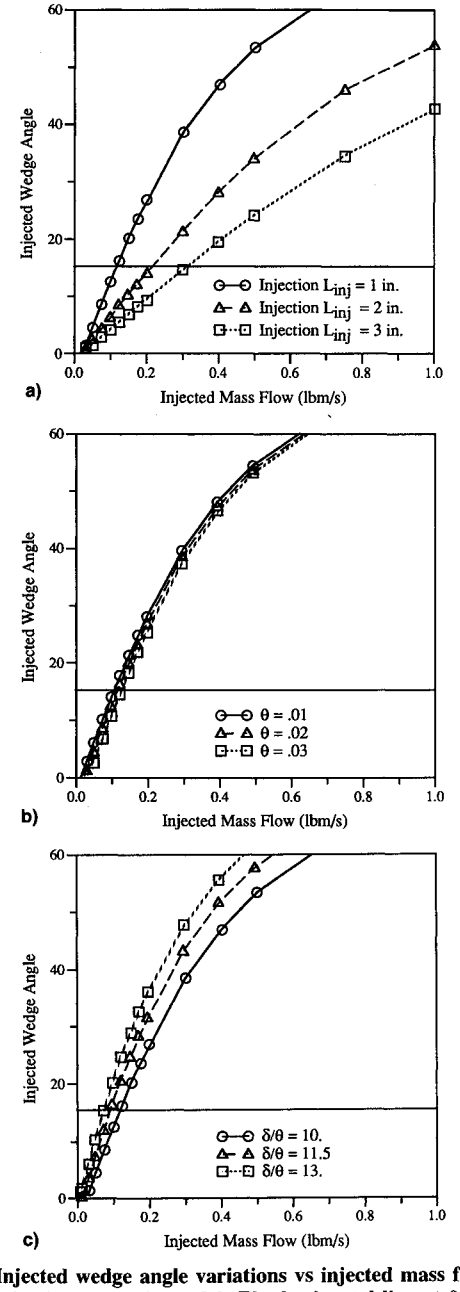

Fig. 2 Injected wedge angle variations vs injected mass flow $\dot{m}$ calculated using Fernandez's model. The horizontal line at 0 = 15 deg represents the limit of Fernandez's theory: a) effect of mass-injection length, b) effect of initial momentum thickness, and c) effect of boundary layer to momentum thickness ratio.

As in Fernandez's experiment, the mass-injection for this study is provided through a side wall already subjected to substantial viscous effects. Calculations using Fernandez's model resulted in predictions much greater than Bott's for a given injected mass flow.[16] The difference between the predictions obtained from both models could be due to the lack of experimental similarity described previously, or to the Mach number and viscous effects, which are not easily quantified.

For Fernandez's model, Fig. 2b indicates that the initial momentum thickness has a limited influence, which decreases rapidly as the mass flow is increased. On the other hand, Fig. 2c indicates that the effects of increasing δ/θ increased with mass flow.

It should be noted at this time that both models are limited to two-dimensional flows and to injected wedge angles smaller than about 15 deg. As noted by Fernandez for his model, above these angles the dividing streamline becomes significantly curved and separation starts occurring at the injection leading edge.

III. Experimental Procedures

This experimental study was conducted using a blow-down wind tunnel in the University of Tennessee Space Institute Gas Dynamics Laboratory. A schematic diagram of the wind-tunnel installations is given in Fig. 3. The wind-tunnel test section consists of an 8- × 8-in.-square duct about 4 ft long. The converging/diverging nozzle has been designed for a test section operating Mach number of 1.8.

The cavity and mass-injection were integrated into the floor plate near the exit of the nozzle as shown in Fig. 3. The cavity was 3.8125 in. long by 1.5 in. wide and 1.5 in. deep. This corresponded to a L/D ratio of 2.54 which belonged to the unattached open cavity flow. This L/D ratio was chosen to provide an open-type cavity flow. It was realized that such a ratio is typically smaller than those found on actual 2.

The injected mass flow was provided through two perforated plates with 175 holes each. Two different hole distributions were studied, each hole diameter was 0.0625 in. and the two arrangements are shown in Fig. 4. The two distribu-

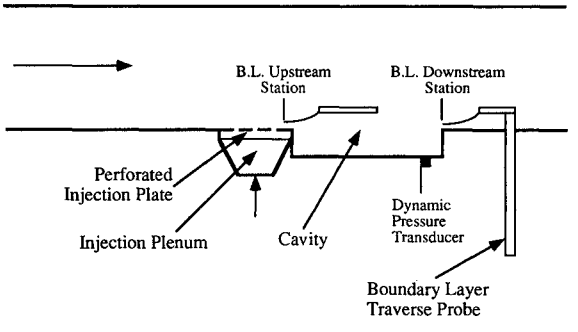

Fig. 3 Schematic of the experimental setup.

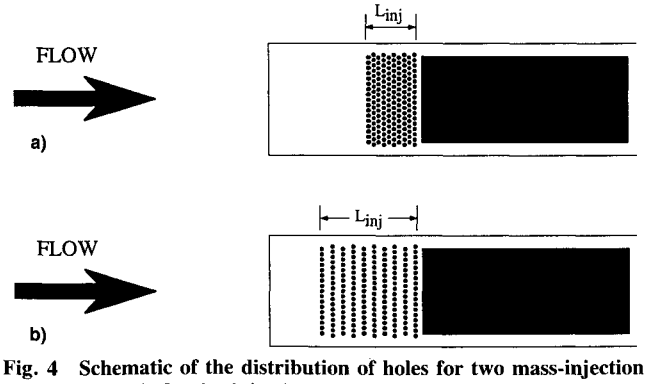

Fig. 4 Schematic of the distribution of holes for two mass-injection systems: a) high-density injection and b) low-density injection.

tions represent one high-density and one low-density porosity, while the total area of injection holes remained constant. The high-density injection area was 1 in. long by 1.75 in. wide, and the low-density injection area was 2.0 in. long by 1.75 in. wide, both were positioned just upstream of the cavity. The injected flow was supplied by a 1-in. pipe into a plenum, just before the perforated plate to enhance the injected flow uniformity. The plenum geometry was sufficiently large for the two perforations and remained fixed.

The cavity flow oscillations were measured using a dynamic pressure transducer installed near the rear of the cavity floor, Fig. 3. The Endevco subminiature piezoresistive pressure transducer model 8514 was connected to a Hewlett Packard model HP3582A frequency spectrum analyzer to provide the amplitudes and frequencies of the cavity oscillations. A spectrum was assembled from 16 samples collected in the frequency range of 0.0–5.0 kHz, with the sampling band width of 30 Hz.

The boundary layer was traversed at two stations, one upstream station, just at the end of injection region near the backward facing step of the cavity, and one in downstream station, just in front of the cavity's rear bulkhead. Velocity profiles were measured using a computer-controlled traversing total pressure probe with a 0.020-in.-thick flattened tip. The reference static pressure for Mach number calculations was on the tunnel floor. Under massive injection, a large normal pressure gradient is believed to exist within the injected flow.[15] Under that condition, the static pressure cannot be assumed to be constant and should be measured directly along with the total pressure using a cone pitot-static probe system. As a result, the velocity profiles obtained with mass-injection were somewhat inaccurate. Nevertheless, to have some qualitative value, the boundary-layer thickness was obtained by neglecting the normal pressure gradient effect.

Numerous static pressures along the tunnel floor were measured by either individual transducers or a 48-channel SCANIVALVE℠.

The injected mass flow was measured using an orifice in the supply line. The injected flow total pressure was measured inside the injection plenum to verify that the flow through the perforated plate was choked.

A schlieren video system provided flow visualization of the tunnel flow, the injected flow, the boundary layer, and the shear layer above the cavity. It was not possible to obtain visual details of the flow inside the cavity with this experimental setup as the optical window did not extend into the cavity.

A. Wind-Tunnel Flow Conditions

The flow in the blowdown tunnel was controlled by throttling the air from a high-pressure storage tank through a control valve. In general, the tunnel Mach number was maintained constant throughout each run and varied within 1% throughout the tests. Similarly, the injected mass flow was maintained constant by continuous control of the injection plenum pressure which was noted to vary slightly during each run. During each run, the tunnel total temperature normally dropped along with the storage tank total temperature and total pressure, due to the throttling of the high-pressure air from the storage tanks. Typical tunnel total conditions were 45 psia and 460°R.

The test section unit Reynolds number Re/ft, was calculated to be 17×10^6 per foot. Komerath et al.[17] reported that the Reynolds number effects are minimal in turbulent cavity flows and should have only a negligible effect on the results. However, the Reynolds number effects may be significant upon the injected flow.

Velocity profiles measured for baseline configuration tests, without any cavity or mass-injection apparatus, at nominal Mach number $M = 1.8$, indicated the boundary-layer thickness was 0.26 in. As observed from the measurements and from the schlieren video, the presence of the cavity resulted in an increase in the shear layer thickness over the cavity.

B. Data Reduction

The local Mach number was calculated from isentropic flow relationships, using total and static pressures. The pitot pressure was corrected for normal shock effects at supersonic Mach numbers. Velocity ratio was calculated using $U/U_e = M/M_e(T/T_e)^{1/2}$, where e indicates conditions at the edge of the boundary layer. A relation between temperature and density for an adiabatic wall was used from Whitfield.[18] The boundary-layer thickness δ is defined as

$$\delta = y|_{U/U_e} = 0.99$$

and other parameters such as δ^*, θ, and H are defined the standard way.

C. Test Procedures

With no cavity installed in the tunnel, without and with mass-injections, baseline measurements were performed to document the test section flow, static pressure distribution along the test section, and the boundary-layer velocity profiles. Then, with the cavity installed, baseline frequencies and amplitudes of cavity oscillations were obtained. Finally, the mass-injection apparatus were installed with the cavity and the effects of mass-injection on the cavity oscillations were documented for various mass-injection rates with the two perforated plates upstream of the cavity. Velocity profiles were also obtained with the cavity installed without and with mass-injection. The presence of cavity resulted in a small increase in the boundary-layer/shear-layer thickness.

IV. Experimental Results

A. Baseline Cavity Oscillations

As indicated in the frequency spectrum in Fig. 5, the amplitudes of oscillations at the peak frequency of 2740 Hz was quite large at 174 dB sound pressure level (SPL), which corresponds to pressure oscillations amplitude of 1.5 psi. Peak cavity oscillations predicted by Rossiter's modified formula, Eq. (2), was around 3100 Hz. Secondary modes or harmonics and 1 were observed at 1360 and 4100 Hz, but with a much smaller amplitude (about 0.15 psi).

B. Effects of Upstream Mass-Injection

The purpose of mass-injection was to control the thicknesses of the boundary layer ahead of the cavity and the cavity shear layer. As indicated by the model as well as the experiment, the injection length (distribution) is a relevant parameter. Hence, to incorporate the distribution of the mass-injection into the analyses, a cavity blowing parameter was introduced. The mass-injection as measured by the cavity blowing parameter is defined as the usual B_c, multiplied by the ratio of the total injection area to the cavity area, $B_c = (\rho_w V_w/\rho_e V_e)(A_{inj}/A_{cavity})$. In this study the cavity blowing pa-

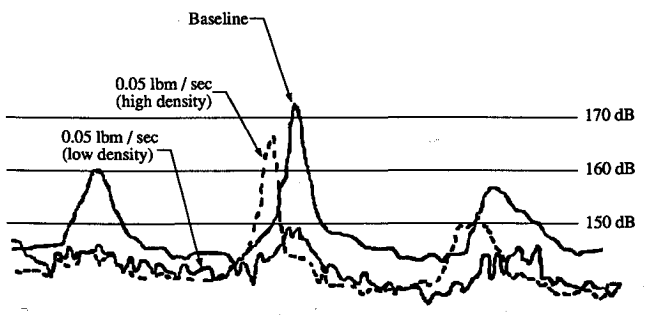

Fig. 5 Typical frequency spectra of the cavity pressure, as indicated by the dynamic pressure transducer (frequency-amplitude spectrum, 0.05 lbm/s).

rameter was varied between 0.0–0.05. Larger cavity blowing parameters could not be obtained without major modifications since the flow was choked in the injection holes and the injection plenum size and maximum pressure was limiting.

The boundary-layer thickness, as observed in the schlieren movie, varied linearly for the lower mass-injection rates and formed a wedge. Measurements at the upstream station, for low- and high-density injections for the flat plate configuration and measurements with the cavity installed, showed that there was some limited upstream influence due to the presence of the cavity. The boundary-layer properties varied with the mass-injection. Maximum thickening of the boundary layer is observed with low-density blowing, Fig. 6. It is noteworthy to remember that low-density injection was from an area twice as long as for high-density injection in the streamwise direction. This may have caused the increased 2 of the boundary layer at the beginning of the cavity. This is consistent with predictions by the model, as shown in Fig. 2.

The mass-injection effect on the cavity shear layer is represented in the boundary-layer traverses at the two stations

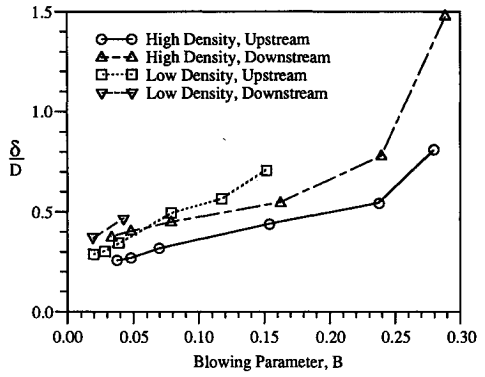

Fig. 6 Effect of blowing on the boundary-layer thickness for high-density and low-density injection patterns.

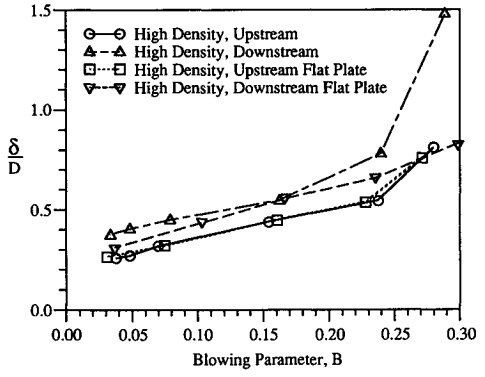

Fig. 7 Comparison of the boundary-layer thickness for the cavity and the flat plate configurations.

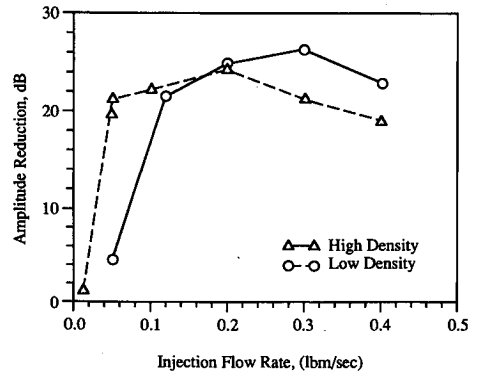

Fig. 8 Attenuation of the cavity's oscillation peak amplitude with mass-injection for two blowing parameters.

as shown in Fig. 6. The thickness of the boundary layer (flat plate configuration) and the shear layer (with the cavity) is also compared at the downstream station in Fig. 7. As shown, there are little or no differences between the two for low blowing coefficients. This indicates that the coupling effect between the shear layer and the cavity has been removed as a result of the thickening of the shear layer. The shear layer on the cavity without blowing was thinner than that with blowing. The relative thickening is consistent with the suppression levels observed. These measurements represent mean values, in general. Large flow curvature and a small region of flow separation was observed over and at the beginning of the blowing area for the higher injection rates. This violated the basic assumptions of the models discussed earlier. For the smaller rates of injection, the flow angles measured (although difficult to establish with good accuracy from the schlieren video) were close to the predictions obtained by Fernandez.

The increase in shear-layer thickness was noted to significantly reduce the amplitude of cavity oscillations from 174 dB (1.5 psi) at 2720 Hz to 147 dB (0.07 psi) at 2530 Hz for the larger injection rates. A shift of about 200 Hz in the peak frequency accompanied the reduction in the amplitude. This shift may be due to the changes in the cavity's effective physical flow properties and dimensions. Figure 8 shows the attenuation of the cavity oscillations for increasing injection rates. The primary frequency peak was reduced by 27 dB, while secondary peaks almost disappeared completely into the background, which was itself reduced by the mass-injection. This reduction of 27 dB in sound pressure level is greater than most attenuation results available, and comparable to one of the most successful,[5] obtaining reductions of 25 dB with significant modifications in the cavity's geometry.

As the mass-injection increased, the amplitude of cavity oscillations sharply decreased at first and leveled off at the larger rates with a small decrease at even higher blowing rates. This is indicated in Fig. 8, which shows that a large reduction can be obtained by relatively small mass-injection rates. The results of Fig. 8 also point out that the thickening of the shear layer is the mechanism for the reduced amplitudes. If mass-injection were blowing the shear layer away and eliminated the interaction, then higher blowing would have to result in a higher reduction in the oscillation amplitudes.

Under massive injection, the cavity shear-layer thickness (and momentum thickness) could be made sufficiently large to prevent any vortex roll-up or any downward deflections of the shear layer, thereby preventing external flow impingement upon the rear corner. Under these conditions, the cavity would appear to be under the minimum length limits established previously by Karamcheti,[19] below which no oscillations occur as the shear layer simply spans the cavity.

The large reduction of cavity oscillations indicates that the physical phenomena which is taking place is that the thickened shear layer spans the cavity with minimum interaction. Thicker shear layers experience a reduction in the organization of their vorticity structures (there is a greater mismatch between its characteristic frequencies and those of the cavity acoustic frequencies), furthermore the feedback is much less effective against the much thicker shear layer.

V. Concluding Remarks

In this study, the effects of upstream mass-injection on cavity flow have been experimentally studied for a cavity with a L/D ratio of 2.54 at a nominal Mach number of 1.8 and for unit Reynolds number of 17×10^6 per foot.

As a result of this study, the following conclusions are drawn:

1) Steady mass-injection increases boundary-layer properties upstream of the cavity, significantly altering the shear layer's instability characteristics and the feedback effectiveness of the cavity's upstream perturbations. This in turn results in a considerable reduction of the cavity oscillations, from 174 dB (1.5 psi) without mass-injection to 147 dB (0.07 psi) at the freestream blowing parameter of $B_e = (\rho_w V_w / \rho_e V_e) =$

0.125, corresponding to a cavity blowing parameter of $B_c = (\rho_w V_w/\rho_e V_e)(A_{inj}/A_{cavity}) = 0.04$.

2) Simple models for a straight wedge injection are limited to very small mass-injections and did not apply, because of the injected flow curvature observed for most of the injection rates used.

3) Low-density injection distribution results in a larger reduction of the pressure oscillations at relatively very low mass flow rates. It is recommended to perform further work to identify the most effective pattern at lowest cavity blowing parameter.

Acknowledgments

This work was supported by the University of Tennessee Space Institute, the Center for Space Transportation and Applied Research, research and proposal preparation funds, and partially by the Air Force Office of Scientific Research. The authors are grateful for the comments and suggestions by the reviewers.

References

[1]Chen, C. H., "Study of Subsonic and Transonic Flow Separation—with and Without Upstream Disturbances," Ph.D. Dissertation, Univ. of Tennessee, Knoxville, TN, March 1975.

[2]Tam, C. R. W., and Block, P. T. W., "On the Tones and Pressure Oscillations Induced by Flow over Rectangular Cavities," *Journal of Fluid Mechanics*, Vol. 89, Pt. 2, 1978, pp. 1373–1399.

[3]Heller, H. H., Holmes, G., and Covert, E. E., "Flow Induces Pressure Oscillations in Shallow Cavities," AFFDL-TR-70-104 (AD-880496), Dec. 1970.

[4]Franke, M. E., and Carr, D. L., "Effect of Geometry on Open Cavity Flow-Induced Pressure Fluctuations," AIAA Paper 75-492, March 1975.

[5]Heller, H. H., and Bliss, D., "The Physical Mechanism of Flow-Induced Pressure Fluctuations in Cavities and Concepts for their Suppression," AIAA Paper 75-491, March 1975.

[6]Sarohia, V., and Massier, P. F., "Control of Cavity Noise," *Journal of Aircraft*, Vol. 14, No. 9, 1977, pp. 833–837.

[7]Franke, M., and Sarno, R., "Suppression of Flow-Induced Pressure Oscillations in Cavities," AIAA Paper 90-4018, Oct. 1990.

[8]Wilcox, F. J., Jr., "Passive Venting System for Modifying Cavity Flow Fields at Supersonic Speeds," *AIAA Journal*, Vol. 26, No. 3, 1988, pp. 374–376.

[9]Wilcox, F. J., Jr., "Experimental Investigation of Porous-Floor Effects on Cavity Flow Fields at Supersonic Speeds," NASA TP-3032, Nov. 1990.

[10]Stallings, R. L., Jr., and Forrest, D. K., private communication, NASA Langley, 1989.

[11]Kim, I., and Chokani, N., "Suppression of Pressure Oscillations in an Open Cavity by Passive Pneumatic Control," AIAA Paper 91-1729, June 1991.

[12]Vakili, A. D., Wu, J. M., and Taylor, M., "Shear Flow Control Applied to Suppress Cavity Oscillations and Improve Store Separation," Weapons Carriage and Separation Workshop, Wright-Patterson AFB, Dayton, OH, April 1988.

[13]Taylor, M., "Cavity Flow Oscillation Analysis and Water Table Simulation," M.S. Thesis, Univ. of Tennessee, Knoxville, TN, Dec. 1989.

[14]Fernandez, F. L., and Zukoski, E. E., "Experiments in Supersonic Flow with Large Distributed Surface Injection," *AIAA Journal*, Vol. 7, No. 9, 1969, pp. 1759–1767.

[15]Bott, J. F., "Massive Blowing Experiments," *AIAA Journal*, Vol. 6, No. 4, 1968, pp. 613–619.

[16]Gauthier, C. R., "Experimental Study of Cavity Flow Oscillations with Mass-Injection," M.S. Thesis, Univ. of Tennessee, Knoxville, TN, Dec. 1990.

[17]Komerath, N. M., Ahuja, K. K., and Chambers, F. W., "Predictions and Measurements of Flows over Cavities—A Survey," AIAA Paper 87-0166, Jan. 1987.

[18]Whitfield, D. L., "Analytical, Numerical, and Experimental Results on Turbulent Boundary Layers," Arnold Engineering Development Center TR-76-62, July 1976.

[19]Karamcheti, K., "Acoustic Radiation from Two-Dimensional Rectangular Cut-Outs in Aerodynamic Surfaces," NACA TN 3487, Aug. 1955.